

General 3D Room Layout from a Single View by Render-and-Compare

Sinisa Stekovic¹

Friedrich Fraundorfer¹

Vincent Lepetit^{2,1}

¹Institute for Computer Graphics and Vision, Graz University of Technology, Graz, Austria

²Université Paris-Est, École des Ponts ParisTech, Paris, France

{sinisa.stekovic, fraundorfer, lepetit}@icg.tugraz.at

Abstract

We present a novel method to reconstruct the 3D layout of a room—walls, floors, ceilings—from a single perspective view, even for the case of general configurations. This input view can consist of a color image only, but considering a depth map will result in a more accurate reconstruction. Our approach is based on solving a constrained discrete optimization problem, which selects the polygons which are part of the layout from a large set of potential polygons. In order to deal with occlusions between components of the layout, which is a problem ignored by previous works, we introduce an analysis-by-synthesis method to iteratively refine the 3D layout estimate. To the best of our knowledge, our method is the first that can estimate a layout in such general conditions from a single view. We additionally introduce a new annotation dataset made of 91 images from the ScanNet dataset and several metrics, in order to evaluate our results quantitatively.

1. Introduction

Estimating the layout of a room is a fundamental problem in scene understanding from images, with potential applications in many domains, such as robotics or augmented reality, as the components of the layout—walls, floors, ceilings—are stable landmarks in comparison to furniture that can be easily moved. With enough images from different views, it is possible to estimate the layout by first building a dense point cloud. This allows to recover complex 3D layouts [1, 15]. In single view scenarios, in the general case, layout components may occlude each other, entirely or partially, which makes recovering the layout very challenging in this case. This rules out approaches based on point cloud processing. Moreover, typical room scenes contain furniture and the view to the walls, the floors and the ceilings might be obstructed. Important image features like corners or edges might be not visible or only partially observable.

As a result, many methods assume that the room is

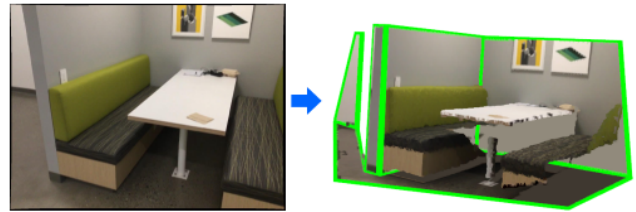


Figure 1: Our method estimates the 3D layout of a room from a single color image even in case of self-occlusions.

a simple 3D cuboid [20, 16, 12, 10, 25, 8, 4]. This is a very strong assumption, which is not valid for many rooms or scenes. In addition, these methods often provide only the 2D projection of the layout in the input image [20, 12, 25, 8], instead of 3D layout, which is not sufficient for many applications. Other methods rely for their input on panoramic images from view points which do not create occlusions [27, 22, 28], which is not always feasible.

In this paper, we introduce a method which recovers a 3D model of the layout from a single perspective view. This view can be an RGB-D image, or even only a color image. When a depth map is not directly available, our method is robust enough to rely on a predicted one from the color image [14, 19]. As shown in Fig. 1, this 3D model is made of a small number of polygons, where each polygon corresponds to one component of the layout. In contrast to recent work [9], our method reasons about intersections of layout components which are partially or entirely occluded in the input image to determine the correct layout, such as the floor and the walls on the left hand side of the input image. This is possible without making strong assumptions on the structure of the layout: Our method only assumes that the layout components are planar. To the best of our knowledge, our method is the first one which can provide a structured layout in the general case from a single perspective view.

Even though applying machine learning to this type of problems is an attractive possibility, we argue that, on its own, it is not enough to tackle this problem. While it is

possible to predict a layout with a 'pure Machine Learning' approach under the assumption that the room is box-shaped [10, 4], it is difficult to have it generalize to general layouts. Moreover, only very limited annotated data is available for the general problem. Nevertheless, machine learning is still useful for extracting image cues on the 3D layout from the perspective view, while geometric reasoning can be utilized in order to adapt to general configurations.

At the core of our method is the definition of a constrained discrete optimization problem which formalizes the problem of recovering a 3D polygonal model of the layout. This optimization selects the polygons which constitute the layout from a large set of potential polygons. To generate these polygons, like some earlier work [17, 9], we rely on 3D planes: Considering planes rather than edges and/or corners keeps the approach simple in terms of perception and model creation. However, as mentioned above, not all 3D planes required in the construction of the layout are visible in the image. We therefore rely on an analysis-by-synthesis approach, sometimes now referred to as 'render-and-compare': We render a depth map for our current layout estimate, and compare it to the measured or predicted depth map. From the differences, we can introduce some of the missing polygons to improve our layout estimate. We iterate this process until convergence.

To evaluate our method, we manually annotated a representative selection of 91 images from the ScanNet [5] dataset, as there was no benchmark for the general problem available. We also introduce 5 different metrics, to evaluate the recovered layouts on three different criteria: Global structure, accuracy in 2D, and accuracy in 3D. We will release our annotations upon publication for comparison with future methods.

In the remainder of the paper, we discuss related work, then describe our method, and its evaluation.

2. Related work

2.1. Layout Generation from Image Features

Most layout generation methods proposed so far attempt to first identify features in the image like room corners or edges, before lifting them into 3D to generate a 3D room layout. The two steps of this approach are, however, very challenging. An assumption used from early on is the Manhattan constraint which enforces orthogonality and parallelism between the layout components of the scene. This was often done by estimating vanishing points [7, 20, 18, 16], a process which can be very sensitive to noise.

Another possible assumption used, which is even stronger than the Manhattan constraint, is that only a single, box-shaped room is visible in the image [20, 16, 12, 25, 8].

For example, in [16], 3D cuboid models are fitted to an edge map extracted from the image, starting from an initial hypothesis obtained from vanishing points. From this 3D cuboid assumption, RoomNet [12] defines a limited number of 10 possible 2D room layout, and trains a CNN to detect the 2D corners of the box-shaped layout. [25] relies on segmentation to identify these corners more robustly. These last approaches [12, 25] are limited to recover a 2D layout, under the cuboid assumption.

Another approach is to directly predict the 3D layout from the image: [10, 4] not only predict the layout but also the objects and humans present in the image, using them as additional constraints. This approach also requires the '3D cuboid assumption', as it predicts the camera pose with respect to a 3D cuboid.

[27, 22, 28] relax the cuboid assumption and can recover more general layouts. However, in addition to the Manhattan assumption, this line of works requires panoramic images which do not exhibit occlusions from walls, which can be difficult or even impossible to guarantee when doing the image capture.

By contrast, our method does not require the cuboid or Manhattan assumptions, and can handle occlusions in the input view.

2.2. Layout Generation from 3D Planes

An alternative to inferring room layouts from image features like room corners is to identify planes in image and infer the room layout from these plane structures. If complete point clouds are available, for example from multiple images, identifying such planes is straightforward. With such data available, plane-based surface reconstruction could be performed like suggested by Nan *et al.* [17] for building reconstruction. From this, a room layout can be generated. Works which directly focus on generating room layouts from point clouds are the work of Cabral and Furukawa [2] and the work of Zhang *et al.* [23]. Recent successes in depth estimation from single image [6, 19, 13] and 3D plane detection and estimation from single image [14] however open up the possibility to use the concept of layout generation from planes in the domain of single image as well.

In fact, only recently a method has been proposed to use these ideas, which makes it closely related to our work: The work of Howard-Jenkins *et al.* [9] utilizes plane detection in single image predicted by a CNN to infer the 3D room layouts, which do not have to be cuboids. The main contribution of their work is in the design of a network architecture to detect planes in single image and to infer the 3D plane parameters from it. Utilizing multiple image frames with known 3D camera poses a 3D representation of the scene composed of planes can be set up. By intersecting these planes, they can be first delineated, and thanks to a clustering and voting scheme, with help of predicted bounding

boxes for the planes, the parts of the planes relevant to the layout can be identified.

Although this work shares similarities to our work, there are significant differences in how the plane information is exploited. The main difference is that our approach can reason about occlusions between layout components in the camera view, which often happens in practice. In addition, we can determine the intersections with the occluded components which are relevant for layout estimation. Furthermore, our method is well formalized and governed by a single discrete optimization problem. Also, while the main experiments in their work focus on evaluating multi-view scenarios for general room layouts, their evaluation of single view scenario is purely on the cuboid NYUv2 303 [24] dataset.

3. Approach Overview

We describe our approach in this section. We first formalize the general layout estimation problem as a constrained discrete optimization problem, explain the way we generate a first set of candidate polygons from plane intersections, and how to find an initial subset of polygons that define the layout. When one or more walls are hidden in the image, this results in an imperfect layout. We then show we can augment the set of candidate polygons to take into account these hidden walls, and iterate until we obtain the final layout.

3.1. Formalization

We formalize the problem of estimating a 3D polygonal layout $\hat{\mathcal{R}}$ for a given input image I as solving the following constrained discrete optimization problem:

$$\hat{\mathcal{R}} = \arg \min_{X \subset \mathcal{R}_0(I)} c(X, I) \quad (1)$$

such that $p(X)$ is a partition of I

where $c(X, I)$ is a cost function defined below, $\mathcal{R}_0(I)$ is a set of 3D polygons for image I , and $p(X)$ is the set of projections in the image of the polygons in X . In words, we look for the subset of polygons in $\mathcal{R}_0(I)$, whose projections partition the input image I , and that minimizes cost function $c(\cdot)$.

There are two options when it comes to defining precisely $c(X, I)$ and $\mathcal{R}_0(I)$: Either $\mathcal{R}_0(I)$ is defined as the set of all possible 3D polygons, and $c(X, I)$ includes constraints to ensure that the polygons in X reproject on image cues for the edges and corners of the rooms, or $\mathcal{R}_0(I)$ contains only polygons with edges that correspond to edges of the room. As discussed in the introduction, extracting wall edges and corners from images is difficult in general, mostly because of lack of training data. We therefore chose the second option. We describe below first how we create the set

$\mathcal{R}_0(I)$ of candidate 3D polygons, which includes the polygons constituting the 3D layout, and then the cost function $c(X, I)$.

3.2. Set of Candidate 3D Polygons $\mathcal{R}_0(I)$

As discussed in the introduction, we rely on the intersection of planes to identify good edge candidates to constitute the polygons of the layout. We then group these edges into polygons to create $\mathcal{R}_0(I)$.

We obtain a first estimate \mathcal{P}_0 of the set of planes on which the polygons lie by detecting planar regions with Plane-RCNN [14] and keeping the regions that correspond to walls, ceilings, or floors, according to a semantic segmentation of the image obtained using DeepLabv3 [3]. Plane-RCNN provides the equations of the 3D planes it detects. If a depth map of the image is available, we fit a 3D plane to each detected region to obtain more accurate parameters. The depth map can be measured or predicted from the input image I [14, 19]. As can be seen in Fig. 2(a), the regions provided by Plane-RCNN typically do not extend to the full polygonal regions that constitute the layout. To find these polygons, we rely on the intersections of the planes in \mathcal{P}_0 as detailed below. In order to limit the extend of the polygons to the borders of the input image, we also include in \mathcal{P}_0 the four 3D planes of the camera frustum. These planes are the planes passing through two neighbouring image corners and the camera center.

Some planes required to create some edges of the layout may not be in this first set \mathcal{P}_0 . This is the case for example for the plane of the hidden wall on the left of the scene in Fig. 2. Through an analysis-by-synthesis approach, we can detect the absence of such planes, and add plausible planes to recover the missing edges and obtain the correct layout. This will be detailed in Section 3.5.

By computing the intersections of each triplet of planes in \mathcal{P}_0 , we obtain a set \mathcal{C}_0 of candidate 3D corners for the room layout. To build a structured layout, it is important to keep track of the planes that generated the corners, and it is thus convenient to represent each corner $C_j \in \mathcal{C}_0$ by a set of 3 different planes:

$$C_j = \{P_j^1, P_j^2, P_j^3\}, \quad (2)$$

where $P_j^1 \in \mathcal{P}_0$, $P_j^2 \in \mathcal{P}_0$, $P_j^3 \in \mathcal{P}_0$, and $P_j^1 \neq P_j^2$, $P_j^1 \neq P_j^3$, and $P_j^2 \neq P_j^3$. For numerical stability, we do not consider the cases where at least two planes are almost parallel, or when the 3 planes almost intersect on a line. We discard the corners that reproject outside the image and those that are behind the depth map for the input image, as they are not visible and thus cannot be part of the visible layout. We also discard those that have negative depth values, as they clearly do not correspond to valid corners.

We then obtain a set \mathcal{E}_0 of candidate 3D edges by pairing

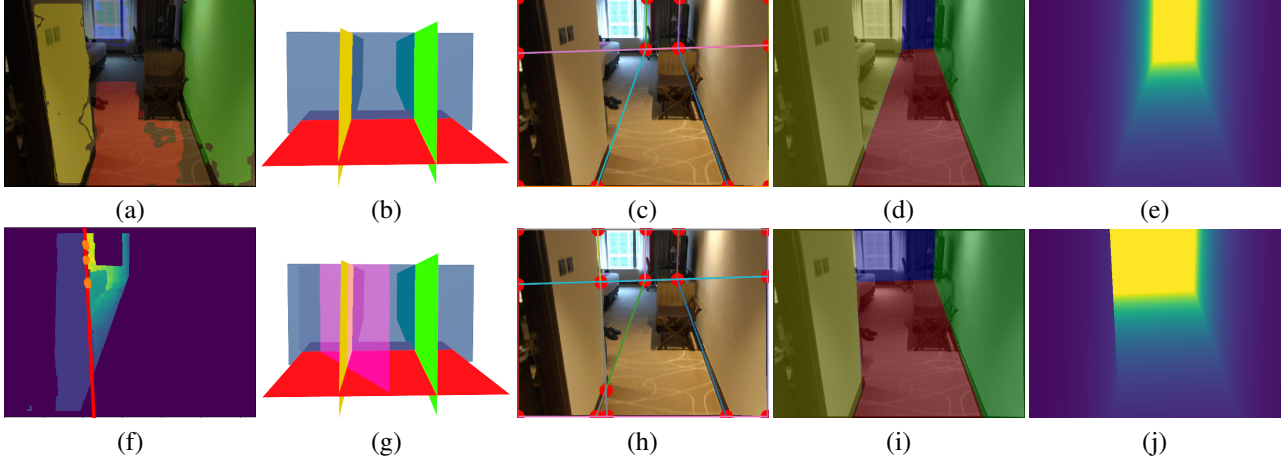


Figure 2: Overview of our approach. We first detect planar regions (a) corresponding to layout components (walls, floors, ceilings) using Plane-RCNN and a semantic segmentation, and obtain the equations of the corresponding 3D planes (b). The intersections between these planes give a set of candidate edges for the final layout (c). Based on these edges, we can find a first estimate of the layout in 2D (d) and 3D (e). From the discrepancy in depth (f) for the layout estimate and the input image, we can identify missing planes and add them (g), to obtain a new set of candidate edges (h). We iterate this process until we find a layout that corresponds to the input image (i) that is consistent in 3D (j).

the corners in \mathcal{C}_0 that share exactly 2 planes:

$$E_k = \{C_{\sigma(k)}, C_{\sigma'(k)}\}, \quad (3)$$

where $\sigma(k)$ and $\sigma'(k)$ are 2 functions giving the indices of the corners that are the extremities of edge E_k . Fig. 2(c) gives an example of such set of candidate edges.

We finally create the set $\mathcal{R}_0(I)$ of candidate polygons as the set of all closed loops of edges in \mathcal{E}_0 that lie on the same plane and do not intersect each other, so that there is no intersection between two edges belonging to the same polygon.

3.3. Cost Function $c(X, I)$

Our cost function is split into a 3D and a 2D part:

$$c(X, I) = c_{3D}(X, I) + \lambda c_{2D}(X, I). \quad (4)$$

For all our experiments, we used $\lambda = 1$.

Cost function $c_{3D}(\cdot)$ measures the dissimilarity with the depth map $D(I)$ for the input image, and the depth map $D'(X)$ created from the polygons in X , as illustrated in Fig. 2(e) for an example. It is based on the observation that the layout should always be located behind the objects of the scene:

$$c_{3D}(I, X) = \frac{1}{|I|} \sum_{\mathbf{x}} \max(D(I)[\mathbf{x}] - D'(X)[\mathbf{x}], 0), \quad (5)$$

where the sum is over all the image locations \mathbf{x} and $|I|$ denotes the total number of image locations.

Cost function $c_{2D}(\cdot)$ measures the dissimilarity between the polygons in the layout and the image segmentation into planar regions:

$$c_{2D}(X, I) = \sum_{R \in X} (1 - \text{IoU}(p(R), M(I, R))) + \text{IoU}(p(R), M(I) \setminus M(I, R)), \quad (6)$$

where IoU is the Intersection over Union score, $p(R)$ is the projection of polygon R in the image, $M(I, R)$ is the planar region detected by Plane-RCNN and corresponding to the plane of polygon R , and $M(I)$ is the set of planar regions detected by Plane-RCNN and corresponding to layout components.

Additionally, we introduce one empty polygon for each of the layout planes with fixed cost $c = 2$ to provide solution when no other solutions are feasible due to the optimization constraints. We found out empirically that this value for the cost balances well throughout our experiments. Such situations are sometimes present when a layout component is completely occluded by another layout component. We still manage to find an optimal solutions for such cases through the iterative layout refinement presented in Section 3.5.

3.4. Optimization

To find the solution to our constrained discrete optimization problem introduced in Eq. (1), we simply consider all the possible subsets X in $\mathcal{R}_0(I)$ that pass the constraints, and keep the one that minimizes cost function $c(X, I)$.

The number N of polygons in $\mathcal{R}_0(I)$ varies with the scene, but is typically of a few tens. For example, we obtain

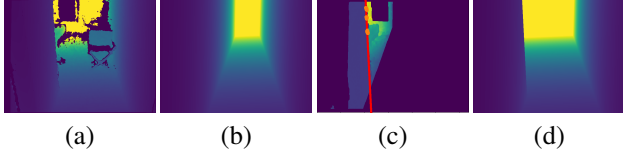


Figure 3: Layout Refinement. We detect planes which are occluded by other layout planes and which are necessary for the computation of the layout. First, we compare the original depth map of the input image (a) to the rendered layout depth (b). (c) If the discrepancy is large, we fit a line (red) through the points with the largest discrepancy change (orange). By computing the plane passing through the line and the camera center, we obtain a layout which is consistent with original depth (d).

12 candidate polygons in total for the example of Fig. 2. The number of non-empty subsets to evaluate is theoretically $2^{(N-1)}$, which is slightly higher than 2000 for the same example. However, most of these subsets can be trivially discarded: Associating polygons with corresponding planes and considering that only one polygon per plane is possible significantly reduces the number of possibilities, to 36 in this example. The number can be further reduced by removing the polygons that do not have a plausible shape to be part of a room layout. Such shapes can be easily recognized by considering the distance between the non-touching edges of the polygon. Finally, this reduces the number to merely 20 plausible subsets of polygons in the case of the example.

3.5. Iterative Layout Refinement

As mentioned above in Section 3.2, we often encounter cases where some of the planes required to create the layout are not in \mathcal{P}_0 because they are hidden by another layout plane. Fortunately, we can detect such mistakes, and fix them by adding a plane to \mathcal{P}_0 before going through the layout creation process described above again.

To detect that a plane is missing, we render the depth map $D'(\hat{\mathcal{R}})$ for the current layout estimate and measure the discrepancy with the depth map $D(I)$ for the image as illustrated in Fig. 3. If the discrepancy is large, *i.e.* there are many pixel location where the rendered map has smaller values than the original depth map, this indicates a mistake in the layout that can be fixed by adding a plane. This is because layout components should never be in front of other objects in the room.

There is a range of planes that can improve the layout estimate. We chose the conservative option that does not introduce parts that are not visible in the input image. For a polygon R in $\hat{\mathcal{R}}$ with a large difference between $D'(\hat{\mathcal{R}})$ and $D(I)$, we first identify the image locations with the largest discrepancy changes, and fit a line to these points

using RANSAC, as shown in Fig. 2 (f). We then add the plane P that passes through this line and the camera center to \mathcal{P}_0 to obtain a new set of planes \mathcal{P}_1 , as illustrated in Fig. 2 (g), since the intersection between P and R will create the edge missing from the layout, as shown in Fig. 2(h). From \mathcal{P}_1 , we obtain successively the new sets \mathcal{C}_1 (corners), \mathcal{E}_1 (edges), and \mathcal{R}_1 (polygons), and solve again the problem of Eq. (1) after replacing \mathcal{R}_0 by \mathcal{R}_1 . We repeat this process until we do not improve the differences between $D'(\hat{\mathcal{R}})$ and $D(I)$, for the image locations segmented as layout components.

For about 5% percent of the test samples, the floor plane is not visible because of occlusions by furniture. When none of the detected planes belongs to the floor class, we create an additional plane by assuming that the camera is 1.5m above the floor. For the plane normal, we take the average of the outer products between the normals of the walls and the $[0, 0, 1]^\top$ vector.

4. Evaluation

We evaluate our approach in this section. First, we present our new benchmark for evaluating 3D room layouts from single images and our metrics. Second, we evaluate our approach on our benchmark and include both quantitative and qualitative results on general room layouts. Finally, we evaluate our approach on the NYUv2 303 benchmark which assumes cuboid layouts and include comparisons to other approaches. Implementation details are given in the supplementary material.

4.1. ScanNet-Layout Benchmark

Dataset creation. As no datasets for evaluating single-view general 3D room layout was available, we created a benchmark dataset we call ScanNet-Layout. We manually annotated 91 representative test scans from the ScanNet test set [5], for testing purposes only. The test samples include both cuboid and more general room layouts, some of them with challenging viewpoints that are often neglected in previous room layout datasets. We will make ScanNet-Layout publicly available for others to compare upon publication.

To manually annotate the 3D layouts, we first drew the layout components as 2D polygons, and for each polygon, the image region where it was directly visible with correct depth values. From these regions, we could compute the 3D plane equations for the polygons. Since we could not recover the plane parameters for completely occluded layout components, we only provide 2D polygons without 3D annotations for them. Annotation examples are provided in the supplementary material.

Evaluation metrics. To enable quantitative evaluation, we introduce several 2D and 3D metrics. For the 2D metrics, we first establish one-to-one correspondences \mathcal{C} between the N predicted polygons $\hat{\mathcal{R}}$ and the M ground truth

polygons \mathcal{R}_{gt} . Starting with largest ground truth polygon, we iteratively find the matching predicted polygon with highest intersection over union value and remove it from the candidate list of predicted polygons for the next iterations. The metrics are:

- Intersection over Union (IoU):

$$\frac{2}{M+N} \sum_{(R_{gt}, R) \in \mathcal{C}} IoU(R_{gt}, R), \quad (7)$$

where IoU is the Intersection-over-Union measure between the 2 polygons. This metric is very demanding and evaluates both the global structure of the layout and its accuracy.

- Pixel Error (PE):

$$\frac{1}{|I|} \sum_{x \in I} PE(x), \quad (8)$$

with $PE(x) = 1$ if $\mathcal{R}(x) = \mathcal{R}_{gt}(x)$ and 0 otherwise, where $\mathcal{R}(x)$ and $\mathcal{R}_{gt}(x)$ are the polygons at pixel location x for the prediction and ground truth sets of polygons respectively. This metric also evaluates the global structure of the layout;

- Edge Error (EE):

$$\frac{1}{2} \sum_{R_{gt} \in \mathcal{R}_{gt}} \sum_{e \in B(R)} DT(\hat{\mathcal{R}})[e] + \sum_{R \in \hat{\mathcal{R}}} \sum_{e \in B(R)} DT(\mathcal{R}_{gt})[e], \quad (9)$$

where $DT(\mathcal{R})[e]$ is the Distance Transform [11] of the boundaries of polygons in \mathcal{R} at pixel location e , and $B(R)$ is the set of pixel locations on the boundary of polygon R . Error EE is therefore the symmetrical Chamfer distance between the contours of the polygons in $\hat{\mathcal{R}}$ and \mathcal{R}_{gt} . This metric evaluates the accuracy of the edges of the layout in 2D;

- Root Mean Square Error (RMSE) between the predicted layout depth $D(\mathcal{R})$ and the ground truth layout depth $D(\mathcal{R}_{gt})$, excluding the pixels that lie on completely occluded layout components, as we could not recover 3D data for these components. This metric evaluates the accuracy of the 3D layout.
- $RMSE_{uts}$ that computes the RMSE after scaling the predicted layout depth to the range of ground truth layout depth by factor $s = \text{median}(D(\mathcal{R}_{gt}))/\text{median}(D(\mathcal{R}))$. This metric is used when the depth map is predicted from the image, as the scale of depth prediction methods is not reliable.

4.2. Evaluation on ScanNet-Layout

We evaluate our method on ScanNet-Layout under two different experimental settings: When depth information is directly measured by a depth camera, and when only the color image is available as input. In this case, we use PlaneRCNN [14] to estimate both the planes parameters and the depth map.

Table 1 reports the quantitative results. Our method shows very high performance when using measured depth. This is because the plane parameters can be estimated reliably from the depth measurements. The performance is best demonstrated by a high value on IoU which has high penalties when components barely visible in the perspective view are missing. Low errors for PE and EE further demonstrate this observation and the value for $RMSE$ demonstrate that our predictions are consistent in 3D as well.

When ground truth depth is not available, the performance decreases due to noisy estimated planes and the depth map from PlaneRCNN. However, in many cases, the predictions are still accurate. This can be best observed in qualitative comparisons with RGBD and RGB views in Fig. 4. In many cases, RGB information is enough to estimate layouts comparable to results with RGBD information. However, the fourth example clearly demonstrates that, even though the planes parameters appear consistent from the estimated layout depth, a small noise in estimated planes parameters can lead to misaligned edges in the final layout. Additionally, we show room layout reconstructions in Fig. 5. The examples illustrates the robustness of our method to handle many different complex layout scenarios, including severe occlusions, occlusions between layout components, and floor that is completely occluded by clutter in the scene.

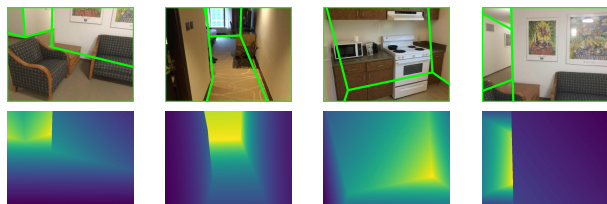
4.3. Evaluation on NYUv2 303

Next, we evaluate our approach on the NYUv2 303 dataset [24, 21], which is a benchmark for evaluating single-view 2D room layouts under the cuboid assumption. We have considered additionally evaluating our approach on the LSUN [26] and the Hedau [7] room layout benchmarks. However, due to missing camera intrinsics and varying image resolutions, we found these datasets unpractical for the evaluation of our approach.

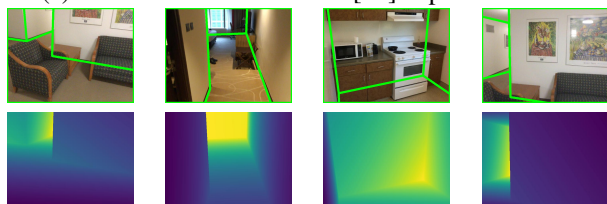
As the NYUv2 303 dataset assumes cuboid shaped room layouts, and only provides annotations for the room corners under this assumption, we relax our method in order to enable quantitative evaluation. In order to do so, for each of the possible layout components—1 floor, 1 ceiling, 3 walls—we find the layout planes for which its normal vector best fits the component of the layout: For example, for the front wall, we pick the closest predicted polygon to be parallel to the image plane. When less than 3 walls are visible, the annotations of walls in the dataset become ambiguous,

Mode	$IoU \uparrow$	$PE \downarrow$	$EE \downarrow$	$RMSE \downarrow$	$RMSE_{uts} \downarrow$
RGBD	72.1 \pm 24.25	10.39 \pm 12.88	10.8 \pm 13.75	0.27 \pm 0.37	0.26 \pm 0.34
RGB	56.19 \pm 23.77	19.22 \pm 14.37	20.2 \pm 12.34	0.64 \pm 0.52	0.46 \pm 0.37

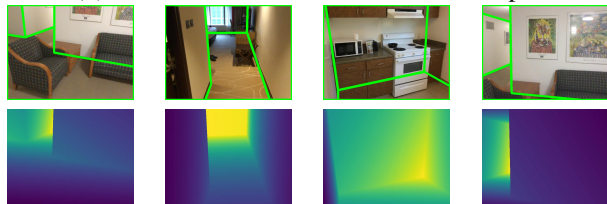
Table 1: Quantitative results on our ScanNet-Layout benchmark. (\uparrow : higher values are better, \downarrow : lower values are better).



(a) RGB mode: PlaneRCNN [14] depth + normals



(b) RGBD mode: Plane normals from depth



(c) ScanNet-Layout annotations and depth Ground Truth

Figure 4: Qualitative comparison of our predicted layouts and predicted depth to the manual annotations in ScanNet-Layout. Our method in (a) and (b) is well aligned with both 2D and 3D annotations from ScanNet-Layout (c). In comparison to our results from RGBD images (b), the estimated layouts from RGB images (a) sometimes show misaligned edges due to noisy plane predictions.

we then apply Hungarian algorithm to assign prediction-to-annotation correspondences of the wall components.

Table 2 gives the quantitative results. When depth is available, we observe that our method is slightly worse than the method of Zhang *et al.* [24]. In comparison to the ScanNet dataset, due to large stereo baseline, depth images have large depth holes in areas close to image boundaries in NYUv2. This limits the performance of our method for some examples, as in these areas, there is not enough information to calculate the layout planes. We experimented with in-filled depths provided with the dataset but such depths disregard planarity, and were not appropriate for our approach.

	Mode	$PE \downarrow$	$Med.PE \downarrow$
Zhang <i>et al.</i> [24]	RGBD	8.04	-
<i>Ours</i> (measured depth)	RGBD	8.9	4.6
Schwing <i>et al.</i> [20]	RGB	13.66	-
Zhang <i>et al.</i> [24]	RGB	13.94	-
RoomNet [12]	RGB	12.31	-
(re-impl. [8])			
Hirzer <i>et al.</i> [8]	RGB	8.49	-
Howard-Jenkins <i>et al.</i> [9]	RGB	12.19	-
<i>Ours</i> (SharpNet [19])	RGB	11.5	6.5

Table 2: Quantitative results on NYUv2 303.

When we consider color images as the only input, we observe that, while planar regions extracted by PlaneRCNN generalize well on the NYUv2 303 dataset, the predicted planes normals tend to be prone to errors. Hence, we use the predicted depth by [19] to estimate the plane parameters. Even though the very recent Hirzer *et al.* [8] is superior to all other benchmarked methods in RGB mode, the relaxed version of our approach still outperforms the other approaches. In fact, we outperform even the method of Howard-Jenkins *et al.* [9], another general room layout method, who similarly relaxed their predictions in order to fit the cuboid shape constraints.

Qualitative results in Fig. 6 compare our method and its relaxed cuboid version. Even though the relaxed version fits the annotations better, our original results correspond better to the actual layouts.

5. Conclusion

We presented what we believe to be to best of our knowledge the first method to estimate a room layout from a single view that does not rely on the cuboid assumption. We notice that the occasional errors made by our method come from the detection of the planar regions, the semantic segmentation, and the predicted depth maps, pointing to the fact that future progress in these fields will improve our layout estimates.

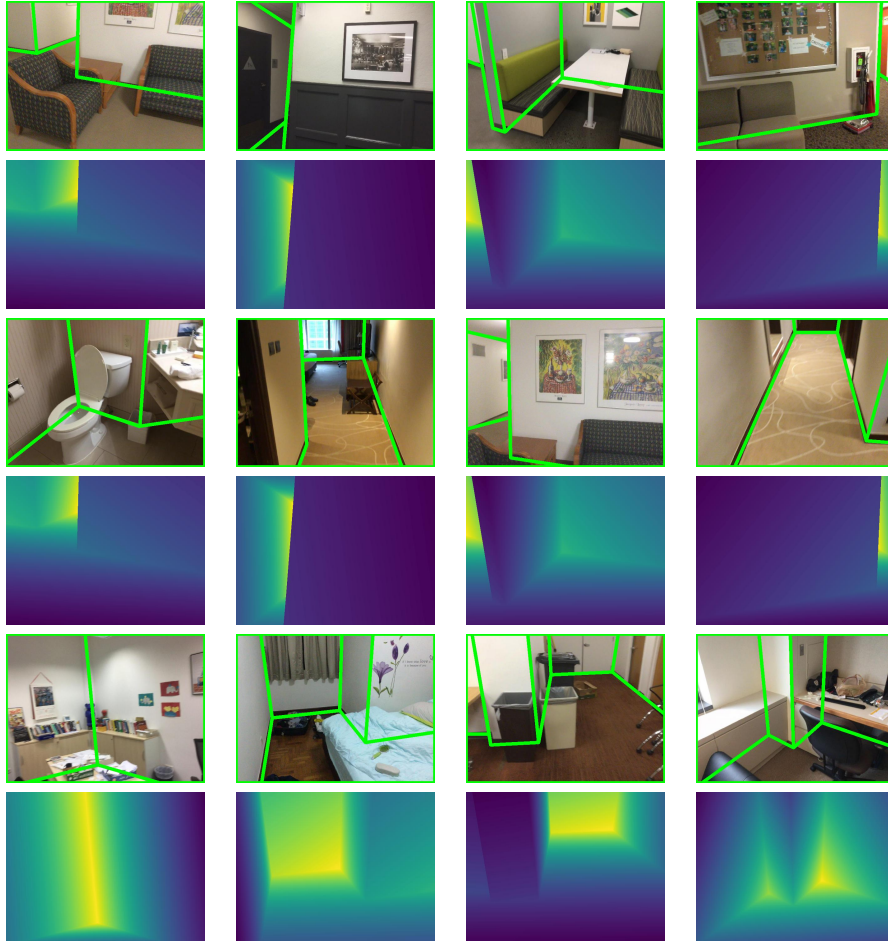


Figure 5: Layouts estimated for images from ScanNet using our method, and the corresponding depths maps.

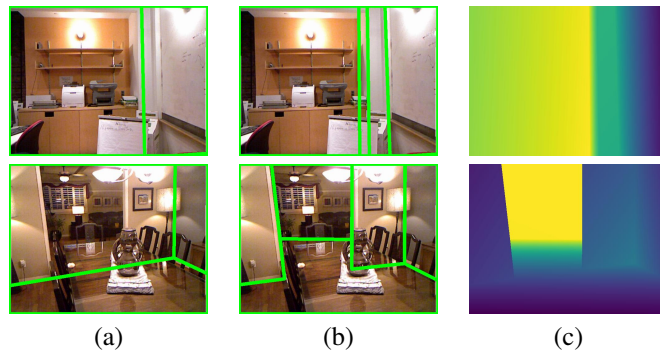


Figure 6: Qualitative results on NYUv2 303. (a) Layouts obtained by enforcing the cuboid assumption, (b) the original layouts retrieved by our method, which correspond better to the scenes. (c) Our estimated layouts in 3D.

Acknowledgment

This work was supported by the Christian Doppler Laboratory for Semantic 3D Computer Vision, funded in part by Qualcomm Inc.

References

- [1] A. Budroni and J. Boehm. Automated 3D Reconstruction of Interiors from Point Clouds. *International Journal of Architectural Computing*, 8(1):55–73, 2010. [1](#)
- [2] R. Cabral and Y. Furukawa. Piecewise Planar and Compact Floorplan Reconstruction from Images. In *Conference on Computer Vision and Pattern Recognition*, pages 628–635, June 2014. [2](#)
- [3] L.-C. Chen, Y. Zhu, G. Papandreou, F. Schroff, and H. Adam. Encoder-Decoder with Atrous Separable Convolution for Semantic Image Segmentation. In *European Conference on Computer Vision*, 2018. [3](#)
- [4] Y. Chen, S. Huang, T. Yuan, S. Qi, Y. Zhu, and S.-C. Zhu. Holistic++ Scene Understanding: Single-View 3D Holistic Scene Parsing and Human Pose Estimation with Human-Object Interaction and Physical Commonsense. In *International Conference on Computer Vision*, 2019. [1, 2](#)
- [5] A. Dai, A. X. Chang, M. Savva, M. Halber, T. Funkhouser, and M. Niessner. Scannet: Richly-Annotated 3D Reconstructions of Indoor Scenes. In *Conference on Computer Vision and Pattern Recognition*, 2017. [2, 5](#)
- [6] C. Godard, O. M. Aodha, and G. J. Brostow. Unsupervised Monocular Depth Estimation with Left-Right Consistency. In *Conference on Computer Vision and Pattern Recognition*, pages 6602–6611, July 2017. [2](#)
- [7] V. Hedau, D. Hoiem, and D. Forsyth. Recovering the Spatial Layout of Cluttered Rooms. In *International Conference on Computer Vision*, 2009. [2, 6](#)
- [8] M. Hirzer, P. M. Roth, and V. Lepetit. Smart Hypothesis Generation for Efficient and Robust Room Layout Estimation. *WACV*, 2020. [1, 2, 7](#)
- [9] H. Howard-Jenkins, S. Li, and V. Prisacariu. Thinking Outside the Box: Generation of Unconstrained 3D Room Layouts. In *Asian Conference on Computer Vision*, pages 432–448, 2019. [1, 2, 7](#)
- [10] S. Huang, S. Qi, Y. Xiao, Y. Zhu, Y. N. Wu, and S.-C. Zhu. Cooperative Holistic Scene Understanding: Unifying 3D Object, layout, and Camera Pose Estimation. In *Advances in Neural Information Processing Systems*, 2018. [1, 2](#)
- [11] Ron Kimmel, Nahum Kiryati, and Alfred M Bruckstein. Sub-pixel Distance Maps and Weighted Distance Transforms. 1996. [6](#)
- [12] C.-Y. Lee, V. Badrinarayanan, T. Malisiewicz, and A. Rabinovich. Roomnet: End-To-End Room Layout Estimation. In *International Conference on Computer Vision*, 2017. [1, 2, 7](#)
- [13] J. H. Lee, M.-K. Han, D. W. Ko, and I. H. Suh. From Big to Small: Multi-Scale Local Planar Guidance for Monocular Depth Estimation. In *arXiv Preprint*, 2019. [2](#)
- [14] C. Liu, K. Kim, J. Gu, Y. Furukawa, and J. Kautz. Planercnn: 3D Plane Detection and Reconstruction from a Single Image. In *Conference on Computer Vision and Pattern Recognition*, 2019. [1, 2, 3, 6, 7](#)
- [15] C. Liu, J. Wu, and Y. Furukawa. Floornet: A Unified Framework for Floorplan Reconstruction from 3D Scans. In *European Conference on Computer Vision*, 2018. [1](#)
- [16] A. Mallya and S. Lazebnik. Learning Informative Edge Maps for Indoor Scene Layout Prediction. In *International Conference on Computer Vision*, 2015. [1, 2](#)
- [17] L. Nan and P. Wonka. Polyfit: Polygonal Surface Reconstruction from Point Clouds. In *International Conference on Computer Vision*, 2017. [2](#)
- [18] S. Ramalingam, J. K. Pillai, A. Jain, and Y. Taguchi. Manhattan Junction Catalogue for Spatial Reasoning of Indoor Scenes. In *Conference on Computer Vision and Pattern Recognition*, 2013. [2](#)
- [19] M. Ramamonjisoa and V. Lepetit. SharpNet: Fast and Accurate Recovery of Occluding Contours in Monocular Depth Estimation. In *International Conference on Computer Vision*, 2019. [1, 2, 3, 7](#)
- [20] A. G. Schwing, T. Hazan, M. Pollefeys, and R. Urtasun. Efficient Structured Prediction for 3D Indoor Scene Understanding. In *Conference on Computer Vision and Pattern Recognition*, 2012. [1, 2, 7](#)
- [21] N. Silberman, D. Hoiem, P. Kohli, and R. Fergus. Indoor Segmentation and Support Inference from RGBD Images. In *European Conference on Computer Vision*, 2012. [6](#)
- [22] C. Sun, C.-W. Hsiao, M. Sun, and H.-T. Chen. Horizonnet: Learning Room Layout with 1D Representation and Pano Stretch Data Augmentation. In *Conference on Computer Vision and Pattern Recognition*, 2019. [1, 2](#)
- [23] J. Zhang, C. Kan, A. G. Schwing, and R. Urtasun. Estimating the 3D Layout of Indoor Scenes and Its Clutter from Depth Sensors. In *International Conference on Computer Vision*, pages 1273–1280, December 2013. [2](#)
- [24] J. Zhang, C. Kan, A. G. Schwing, and R. Urtasun. Estimating the 3D Layout of Indoor Scenes and Its Clutter from Depth Sensors. In *International Conference on Computer Vision*, 2013. [3, 6, 7](#)
- [25] W. Zhang, W. Zhang, and J. Gu. Edge-Semantic Learning Strategy for Layout Estimation in Indoor Environment. *IEEE Transactions on Cybernetics*, 2019. [1, 2](#)
- [26] Y. Zhang, F. Yu, S. Song, P. Xu, A. Seff, and J. Xiao. Large-Scale Scene Understanding Challenge: Room Layout Estimation. 2016. [6](#)
- [27] C. Zou, A. Colburn, Q. Shan, and D. Hoiem. LayoutNet: Reconstructing the 3D Room Layout from a Single RGB Image. In *Conference on Computer Vision and Pattern Recognition*, 2018. [1, 2](#)
- [28] C. Zou, J.-W. Su, C.-H. Peng, A. Colburn, Q. Shan, P. Wonka, H.-K. Chu, and D. Hoiem. 3D Manhattan Room Layout Reconstruction from a Single 360 Image. In *arXiv Preprint*, 2019. [1, 2](#)

General 3D Room Layout from a Single View by Render-and-Compare - Supplementary Material

Sinisa Stekovic¹

Friedrich Fraundorfer¹

Vincent Lepetit^{2,1}

¹Institute for Computer Graphics and Vision, Graz University of Technology, Graz, Austria

²Université Paris-Est, École des Ponts ParisTech, Paris, France

{sinisa.stekovic, fraundorfer, lepetit}@icg.tugraz.at

1. Implementation details

1.1. Handling Noisy Observations

We have presented our method under assumptions that the initial estimations of planar regions, semantic segmentation and depth map are perfectly extracted from the input image. In practice, however, this is not the case. We empirically choose the hyper-parameters that generalize well across many images of our ScanNet-Layout benchmark and perform the following steps to handle noisy observations:

- We consider a planar region, predicted by PlaneRCNN, to be part of the layout only if more than 0.4 pixels locations of the plane belong to one of the layout categories—wall, floor, ceiling.
- After calculating the planes parameters using RANSAC, we discard planes that are inconsistent with the depth map for the input image across the corresponding planar region. If the number of outliers during the RANSAC procedure is larger than 0.3, we discard the corresponding plane. As outliers, we consider the points with distance larger than 0.01 to the fitted plane. When planes parameters are predicted using PlaneRCNN, we skip this step.
- PlaneRCNN might falsely predict multiple planar regions in place of one. In order to handle such mistakes, we merge layout planes that are parallel and have similar camera offset, up to some threshold values. In case of RGBD image as input, we set both of these hyper-parameters to 0.3. When using RGB image as input, to compensate for the noise in plane estimation, we set these parameters to 0.5 and 0.6 respectively. However, it is also possible that given scene consists of multiple layout components with same plane parameters. Hence, we merge the planes only if they are neighbouring layout planes. In other words, there are no other planar regions from M_L in-between them. For

the merged planes, the new parameters are simply calculated as a mean of the two planes.

- Layout refinement is performed only if discrepancy between the rendered layout depth and the depth map for the input image is larger than a threshold value for at least 1000 image locations. We set this threshold value to 0.1 when utilizing measured depth, and 0.5 for predicted depths.
- Even though one might consider discarding invalid depth values completely from all calculations, we found that processing depth with a depth completion method [4] is important during iterative layout refinement. Depth holes often appear around edges in the image. This can be problematic when performing line fitting for the refinement stage as the pixels locations with highest magnitude of change in discrepancy might be missing. We found that comparing depth from planes to filled depth improves accuracy of the refined layout.

1.2. Networks details

For all networks, we consider input image resolution of 640×480 . PlaneRCNN [5] is the original network that was pre-trained on the ScanNet dataset [2] by the authors. We train DeepLabV3+ [1] on the SUNRGB-D dataset [9], a collection of datasets, made of an original dataset and additional datasets previously published [7, 3, 10]. For SharpNet [6], we use the set of weights pre-trained on the NYUv2 dataset [11, 8].

2. Run-Time

In Table 1 we present the run-time of our approach. As we do not optimize the run-time performance, except for the network predictions, that run on NVIDIA GeForce 1080 Ti, all other components are implemented to run on a single CPU. As the run-time differs based on the number of

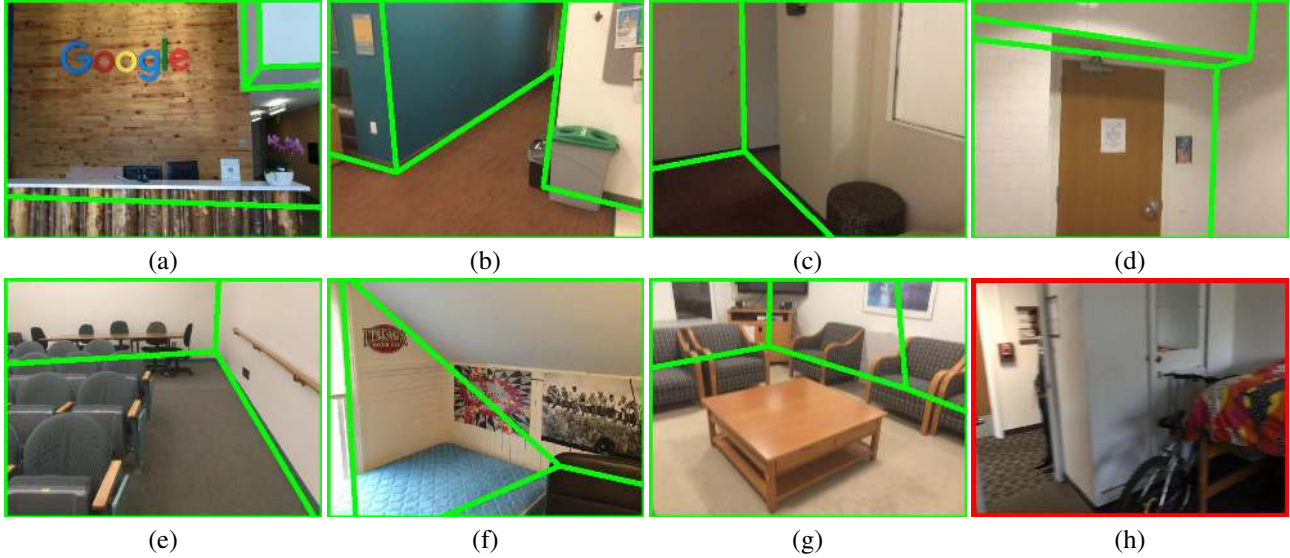


Figure 1: Failure cases. (a) With increased distance from the camera, depth measurements become very noisy and sparse. Hence, our method fails to detect the corridor in the right part of the image. (b), (c), (d), (e) Show failure cases when layout planes are not detected correctly, due to noisy semantic segmentation or missing planar regions. (f) shows a failure case when floor is not visible and the assumption about the height of the camera is incorrect. (g) Demonstrates a failure case when estimated planes parameters are not parallel and, therefore, cannot be merged. (h) Shows an example where our approach does not find a feasible solution as none of the subsets of candidate polygons fulfils the optimization constraints.

	Time (s)
Networks Predictions	< 0.3
Fitting Layout Planes with RANSAC	8.2
Finding Candidate Edges	0.08
Optimal Polygon Search	1.26
Iterative Refinement	3.12

Table 1: Run-time performance.

estimated layout components, we compute the average run-time across the images of our ScanNet-Layout benchmark.

Depending on the networks that are utilized during inference for different scenarios, the run-time slightly varies, but the time for network predictions never exceeds 0.3s. Most notably, the bottleneck of our computations is during the plane fitting step that, we strongly believe, can be further optimized. When using PlaneRCNN to estimate the plane parameters, this step is completely ignored.

3. Failure Cases

Fig. 1 shows failure cases on ScanNet-Layout benchmark.

4. ScanNet-Layout Results

We show results on all of the 91 images from our ScanNet-Layout benchmark in Fig. 2, 3, 4, 5.



Figure 2: (Part 1) ScanNet-Layout benchmark. For each sample, first row are the 2D annotations, second row are the results with RGBD input, third row are the results with RGB input. Predictions outlined with red rectangle are the ones that our approach finds infeasible.

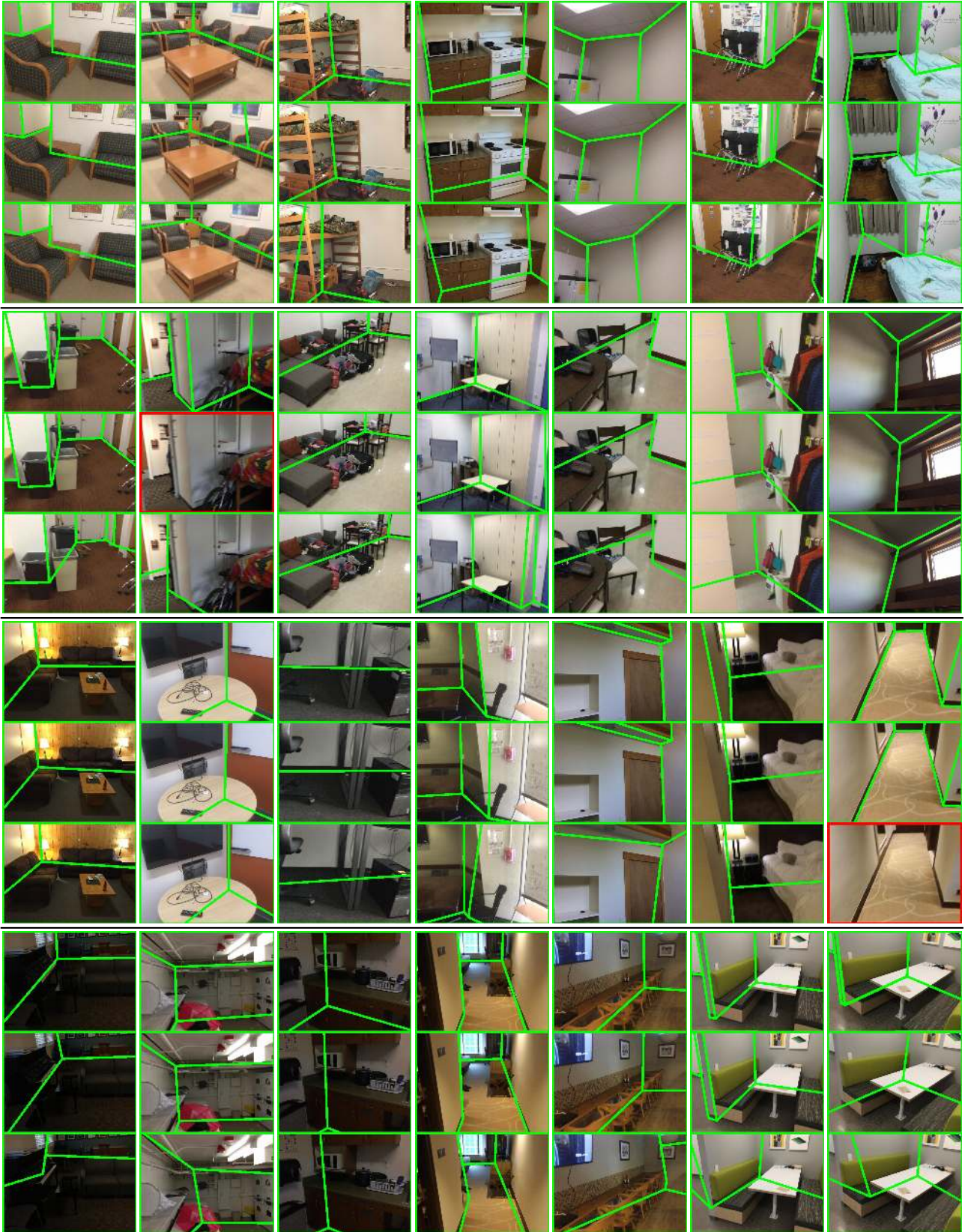


Figure 3: (Part 2) ScanNet-Layout benchmark. For each sample, first row are the 2D annotations, second row are the results with RGBD input, third row are the results with RGB input. Predictions outlined with red rectangle are the ones that our approach finds infeasible.



Figure 4: (Part 3) ScanNet-Layout benchmark. For each sample, first row are the 2D annotations, second row are the results with RGBD input, third row are the results with RGB input. Predictions outlined with red rectangle are the ones that our approach finds infeasible.

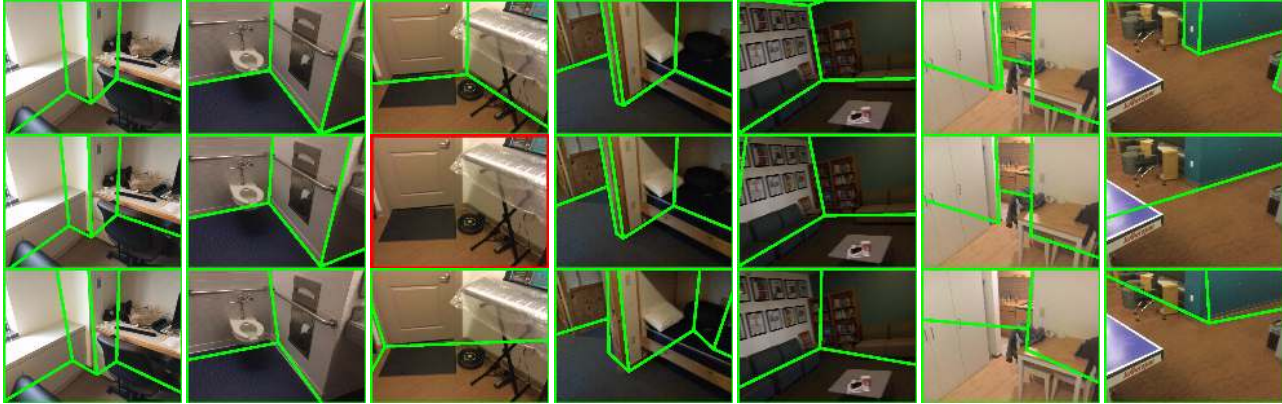


Figure 5: (Part 4) ScanNet-Layout benchmark. For each sample, first row are the 2D annotations, second row are the results with RGBD input, third row are the results with RGB input. Predictions outlined with red rectangle are the ones that our approach finds infeasible.

References

- [1] L.-C. Chen, Y. Zhu, G. Papandreou, F. Schroff, and H. Adam. Encoder-Decoder with Atrous Separable Convolution for Semantic Image Segmentation. In *European Conference on Computer Vision*, 2018. 1
- [2] A. Dai, A. X. Chang, M. Savva, M. Halber, T. Funkhouser, and M. Niessner. Scannet: Richly-Annotated 3D Reconstructions of Indoor Scenes. In *Conference on Computer Vision and Pattern Recognition*, 2017. 1
- [3] Allison Janoch, Sergey Karayev, Yangqing Jia, Jonathan T Barron, Mario Fritz, Kate Saenko, and Trevor Darrell. A Category-Level 3D Object Dataset: Putting the Kinect to Work. In *Consumer Depth Cameras for Computer Vision*. 2013. 1
- [4] J. Ku, A. Harakeh, and S. L. Waslander. In Defense of Classical Image Processing: Fast Depth Completion on the CPU. In *CRV*, 2018. 1
- [5] C. Liu, K. Kim, J. Gu, Y. Furukawa, and J. Kautz. Planercnn: 3D Plane Detection and Reconstruction from a Single Image. In *Conference on Computer Vision and Pattern Recognition*, 2019. 1
- [6] M. Ramamonjisoa and V. Lepetit. SharpNet: Fast and Accurate Recovery of Occluding Contours in Monocular Depth Estimation. In *International Conference on Computer Vision*, 2019. 1
- [7] Nathan Silberman, Derek Hoiem, Pushmeet Kohli, and Rob Fergus. Indoor Segmentation and Support Inference from RGBD Images. In *ECCV*, 2012. 1
- [8] N. Silberman, D. Hoiem, P. Kohli, and R. Fergus. Indoor Segmentation and Support Inference from RGBD Images. In *European Conference on Computer Vision*, 2012. 1
- [9] S. Song, S. P. Lichtenberg, and J. Xiao. SUN RGB-D: A RGB-D Scene Understanding Benchmark Suite. In *Conference on Computer Vision and Pattern Recognition*, 2015. 1
- [10] Jianxiong Xiao, Andrew Owens, and Antonio Torralba. SUN3D: A Database of Big Spaces Reconstructed Using SfM and Object Labels. In *ICCV*, 2013. 1
- [11] J. Zhang, C. Kan, A. G. Schwing, and R. Urtasun. Estimating the 3D Layout of Indoor Scenes and Its Clutter from Depth Sensors. In *International Conference on Computer Vision*, 2013. 1